AIAA JOURNAL
Vol. 48, No. 1, January 2010

Piezoelectric Control of a Partially Propped Cantilever Subjected to a Follower Force

Sunjung Kim* and Srinivasan Sridharan†
Washington University in St. Louis, St. Louis, Missouri 63130

DOI: 10.2514/1.42536

A cantilever column carrying a compressive follower force and propped by a spring can become dynamically unstable by flutter or divergence depending upon spring stiffness. In this study, issues involved in the control of such a column by means of piezoelectric patches at the top and bottom surfaces of the column are studied. Attention is focused on negative feedback control with patch voltages proportional to the locally sensed bending strain rates. It is found such control is capable of significantly enhancing the critical load in the flutter range, such enhancement being limited often only by the limits on voltage developed across the patch of given thickness. In the range of spring stiffness corresponding to buckling failure, this control strategy is simply ineffective. A relatively light spring not only enhances the critical force significantly but also makes the control more effective. For prescribed limits on voltage across the patch, there is an optimal spring stiffness that results in the maximum of critical load and this lies in the flutter range of the spring stiffness. Softening nonlinearity reduces the critical loads in the range of transition from flutter to divergence and rounds off the sharpness of the drop in this range seen in the linear case. A partial patch spanning over half the length of the column from the fixed end is significantly more effective than a full patch in the flutter range.

Nomenclature

b	=	b_P, width of the column section (width of piezoelectric patch)
E	=	Young's modulus of the material of the host beam
E_P	=	Young's modulus of the piezoelectric material
e_P	=	piezoelectric constant
H	=	depth of the column section
G	=	control gain
K_1, K_3	=	spring constants
I	=	second moment of the area about the weaker axis
L	=	length of the beam
$\bar{m}$	=	mass per unit length of the column
N	=	number of harmonics in the Fourier series description
P	=	axial (compressive) load
P_E	=	Euler buckling load of a column with pinned ends, $\pi^2 EI/L^2$
P_{cr}	=	critical load as determined from linear stability analysis
$P_{\max}$	=	maximum load attained by the column for a give gain
q_o	=	uniformly distributed lateral load per unit length
V	=	voltage across the piezoelectric patch
V_m	=	mth coefficient in the Fourier series representation of V
v	=	lateral displacement of the column
v_m	=	mth coefficient in the Fourier series representation of v
$\bar{v}_m$	=	v_m/L
β_1, β_3	=	nondimensional linear and nonlinear spring stiffnesses, respectively

Received 3 December 2008; revision received 18 September 2009; accepted for publication 21 September 2009.

*Graduate Student, Mechanical, Aerospace & Structural Engineering, One Brookings Drive, Box 1185; sk13@cec.wustl.edu.

†Professor, Mechanical, Aerospace & Structural Engineering, One Brookings Drive, Box 1185; ssrid@seas.wustl.edu. Senior Member AIAA.

I. Introduction

THE control of flutter and divergence (static buckling) of slender structures is an important problem in the design and operation of aerospace structures. There have been numerous publications that deal with piezoelectric control of flutter and buckling of simple columns [1–6], plates subjected to lateral disturbances [7–9] as well as aircraft wings undergoing flutter because of aerodynamic pressure acting on them [10,11]. With a view to gain an insight into the key issues in the control of complex structures used in practice, a relatively simple structure is examined in this paper. The problem considered is that of a cantilever column carrying a compressive follower force and propped by a spring at its free end. The type of control considered is negative feedback control with voltages proportional to the bending strain rates (proportional to velocity) sensed at the top and bottom of the longitudinal surfaces of the column. This type of control is selected as it is the most energy-efficient in that it comes into effect only when it is needed and ceases as soon as the induced vibrations are damped out. This is in contrast to the strategy proposed by Wang and Quek [1] and Wang [6], who considered a type of piezoelectric control that was tantamount to pretensioning the column. Depending upon the tension applied, the critical load can be enhanced to any desired extent. The disadvantage of this technique is that energy must be constantly supplied during the life of the column and is apt to be expensive and is not therefore pursued here. Because the suppression of vibration is the principal desideratum in aerospace applications, a velocity dependent feedback rather than displacement dependent feedback is selected, notwithstanding the fact the latter can enhance the buckling load [2]. The latter also results in residual field strengths that must be maintained if the column were to settle in a bent equilibrium configuration because of, say, some lateral pressure.

The problem of the cantilever column subjected to follower force is a simplified structural model of a flexible rocket, missile, or spacecraft [12] and hence is of technical interest. It is shown in the present paper that the critical load corresponding to flutter of such a column can be significantly enhanced by 1) a partial propping of the free end by a spring: a passive design feature and 2) piezoelectric actuation proportional to bending strain rate: an active control technique. However, any softening nonlinearity in the spring would appreciably cut into the expected enhancements in the critical load and hence is considered in the present study.

After a brief presentation of the formulation employed, the relationship between the critical load and the spring stiffness is

presented in the linear as well as the nonlinear case. (Note that such a relationship has already been presented by Wang and Quek [1] for the linear case.) The spring nonlinearity has a dramatic effect of rounding of the sharp drop in this relationship in the range of transition from flutter to buckling. The possibility of piezoelectric actuation in enhancing the critical load as well as its effectiveness in damping out the vibrations below the critical load are investigated with spring nonlinearity taken into account. This is followed by a study of piezoelectric control with a patch that covers only a part of the column from the fixed end. It is seen that a partial patch does have a performance that is superior to that of a full patch covering the entire column. The paper concludes by highlighting the major findings of the investigation.

II. Theoretical Formulation and Solution Procedure

The present analytical treatment is based on the familiar assumptions of the Euler–Bernoulli beam theory. Thus, the effects of shear deformation and rotary inertia are neglected, as we are considering beams whose depth is small compared to the length. The displacements are assumed to be small but finite. The centroidal axis of the column does not stretch under bending.

Figure 1 shows the column AB clamped at A ($x = 0$) and supported by a spring at B ($x = L$). The deformation of the column under foregoing assumptions is defined by v, the lateral displacement of the column. The spring is deemed to be elastic and nonlinear, and has the following force displacement relationship:

$$F = K_1\delta + K_3\delta^3 \quad \text{where } \delta = v|_{x=L} \tag{1}$$

The equation of motion for the beam is written using the principle of virtual work.

A. External Virtual Work

1. Inertial Term

$$-\int_0^L \bar{m}\,\ddot{v}\,\delta v\,\mathrm{d}x \tag{2}$$

where $\bar{m}$ is the mass per unit length, v is the lateral displacement, L is the length of the beam, and a dot denotes differentiation with respect to time.

2. Contribution of the Axial Force

$$-P\delta u|_{x=L} - P\frac{\mathrm{d}v}{\mathrm{d}x}\delta v\bigg|_{x=L} \tag{3}$$

where u is the axial displacement along the centroidal axis. Note that the second term is due to the follower nature of the axial force. Because of in-extensionality,

$$\varepsilon = \frac{\mathrm{d}u}{\mathrm{d}x} + \frac{1}{2}\left(\frac{\mathrm{d}v}{\mathrm{d}x}\right)^2 = 0 \tag{4}$$

with $u = 0$ at $x = 0$,

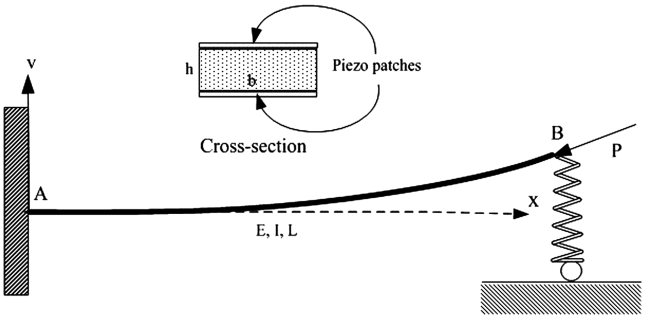

Fig. 1 The cantilever column with a spring under follower force together with a cross section of the column.

$$u|_{x=L} = -\frac{1}{2}\int_0^L \left(\frac{\mathrm{d}v}{\mathrm{d}x}\right)^2 \mathrm{d}x \tag{5}$$

so that,

$$\delta u|_{x=L} = -\int_0^L \left(\frac{\mathrm{d}v}{\mathrm{d}x}\right)\left(\frac{\mathrm{d}\delta v}{\mathrm{d}x}\right)\mathrm{d}x \tag{6}$$

Thus, Eq. (3) can be written in the form

$$P\int_0^L \left(\frac{\mathrm{d}v}{\mathrm{d}x}\right)\left(\frac{\mathrm{d}\delta v}{\mathrm{d}x}\right)\mathrm{d}x - P\frac{\mathrm{d}v}{\mathrm{d}x}\delta v|_{x=L} \tag{7}$$

Add to this a contribution from any distributed lateral load $q(x)$ acting on the beam at any instant. The corresponding external virtual work contribution is

$$\int_{x=0}^L q(x)(\delta v)\mathrm{d}x \tag{8}$$

B. Internal Virtual Work of the Host Beam

1. Internal Virtual Work Associated with Bending

This is numerically equal to the first variation of bending energy and may be written in the form

$$EI\int_0^L \frac{\mathrm{d}^2 v}{\mathrm{d}x^2}\frac{\mathrm{d}^2\delta v}{\mathrm{d}x^2}\mathrm{d}x \tag{9}$$

2. Contribution from the Spring

$$\{(K_1 v + K_3 v^3)\delta v\}_{x=L} \tag{10}$$

C. Contribution from Piezoelectric Patches

The piezoelectric constitutive equations take the form [13,14]

$$T_{ij} = c^E_{ijkl}S_{kl} - e_{kij}E_k \tag{11a}$$

$$D_i = e_{ikl}S_{kl} + \varepsilon^S_{ij}E_k \tag{11b}$$

where T_{ij} and D_i are the stress components and electric displacement, respectively; S_{kl} and E_k are the kinematic strains and electric field intensity, respectively; and c^E_{ijkl}, e_{kij}, and ε^S_{ij} are the elastic, piezoelectric, and dielectric constants, respectively. The electric enthalpy density H is defined by

$$H = H(S_{kl}, E_k) = U - E_i D_i = \frac{1}{2}c^E_{ijkl}S_{ij}S_{kl} - e_{kij}E_k S_{ij} - \frac{1}{2}\varepsilon^S_{ij}E_i E_j \tag{12}$$

The virtual work contribution per unit volume is numerically equal to the first variation of H (i.e., δH).

Consider a column with thin piezoelectric patches attached to its top and bottom surfaces and let the voltage across the patch be prescribed. If the patches are sufficiently thin, the field strength and the strain may be assumed to be constant across them. Thus, from Eq. (11b), the charge equation of electrostatics ($D_{i,i} = 0$) is automatically satisfied. Further, for an actuator patch, we assume that the accumulated charges given by Eq. (11b) do not affect the piezoelectric constants e_{kij} (linear behavior). Consequently, Eq. (11b) becomes defunct and does not need to be considered any further. Because the voltages are prescribed over the patches and the variation of electric field strengths must be set to zero, the electric enthalpy variation may be taken in the truncated form

$$\delta H = c^E_{ijkl}S_{kl}\delta S_{ij} - e_{kij}E_k\delta S_{ij} \tag{13}$$

Note also that the variation of surface charges are zero and the corresponding term in the external virtual work [i.e., $(\bar{\sigma} + n_i D_i)\delta\phi$] also vanishes [13]. Because we are considering a beam problem, the

stress and strain in the longitudinal direction alone are significant. Thus, Eq. (13) takes the form

$$\delta H = E_p\left(\varepsilon_p - e_p\frac{V}{t_p}\right)\delta\varepsilon_p = E_p\varepsilon_p\delta\varepsilon_p - E_p e_p\frac{V}{t_p}\delta\varepsilon_p \tag{14}$$

where the subscript p refers to the piezoelectric material, E_P is the Young's modulus in the longitudinal direction, e_p is the relevant piezoelectric constant for voltage applied in the transverse direction [15] (d_{31}) and t_P is the patch thickness. The first term in Eq. (14) is purely mechanical and the second term is the electromechanical coupled term.

D. Electromechanical Coupled Term

To control bending, let the beam be actuated by identical piezoelectric patches attached to the top and bottom surfaces, respectively, of the beam with voltages equal in magnitude but opposite in sign. As the bending strains suffered by the patches at the top and bottom are equal and opposite, so are the electric field strengths across them. The virtual bending strains in the piezoelectric material (denoted by the subscript p) take the form

$$\delta\varepsilon_p|_{Z=\pm\frac{h}{2}} = \mp\frac{h}{2}\cdot\frac{\mathrm{d}^2(\delta v)}{\mathrm{d}x^2} \tag{15}$$

where h is the depth of the column measured center to center of the piezoelectric patches at the top and bottom. The coupled internal virtual work contribution from the double piezoelectric patches is then

$$\delta W^c_{\text{int}} = 2E_p e_p\frac{h}{2}b_p\int_x V(x)\frac{\mathrm{d}^2(\delta v)}{\mathrm{d}x^2}\mathrm{d}x \tag{16}$$

Note the integration is over the patches which may be continuous or discrete. Very significantly, the thickness t_p disappears in Eq. (16) as it gets canceled under integration over the volume of the patches.

E. Mechanical Work Term

Now consider the mechanical internal work contribution from Eq. (14). To evaluate this term we need an a priori estimate of the thickness of the patch(es). If the piezoelectric patch is sufficiently thin, we may neglect the corresponding mechanical work term altogether without any serious error (or absorb it in the internal work

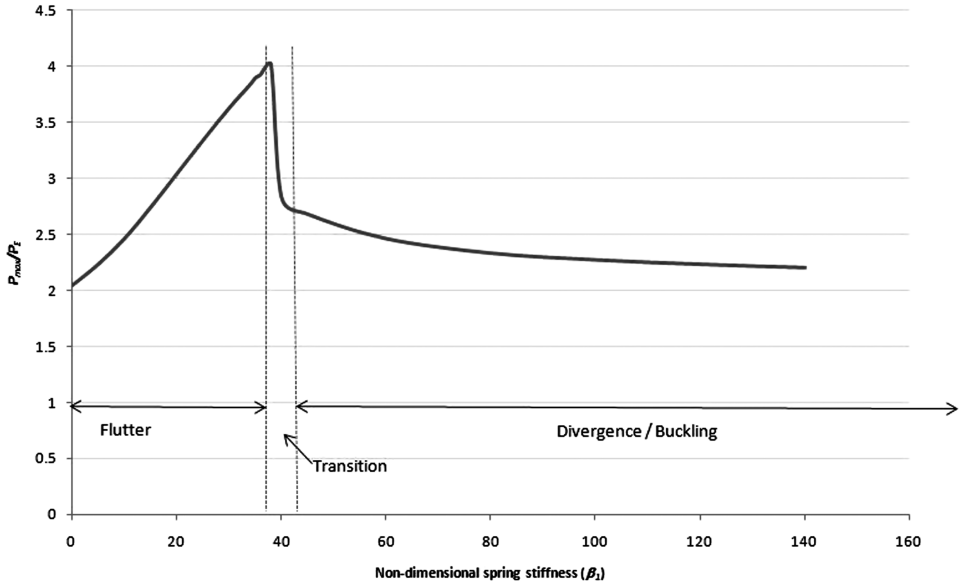

Fig. 2 Critical limits of $P_{\max}/P_E$ versus nondimensional spring coefficient, β_1.

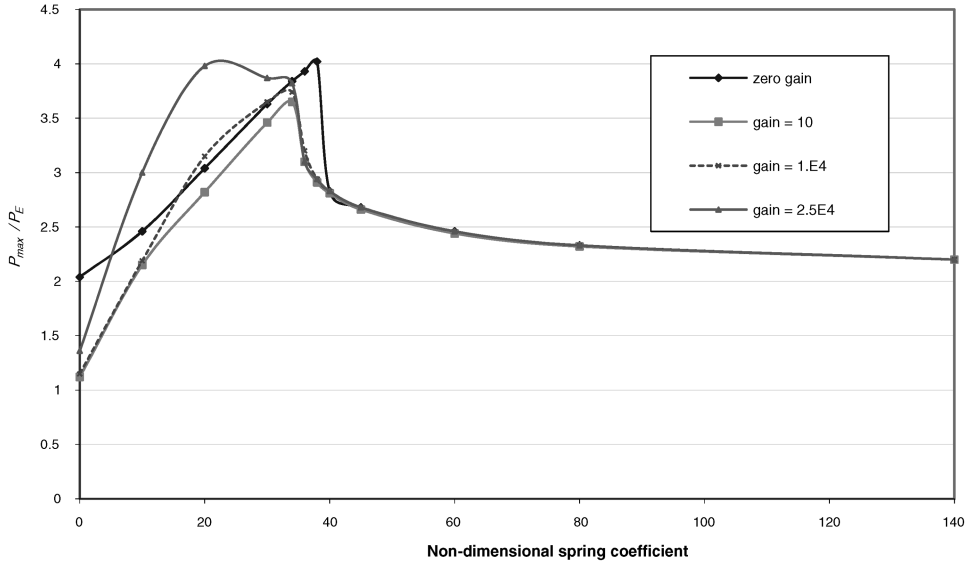

Fig. 3 Variation of maximum $P_{\max}/P_E$ with β_1.

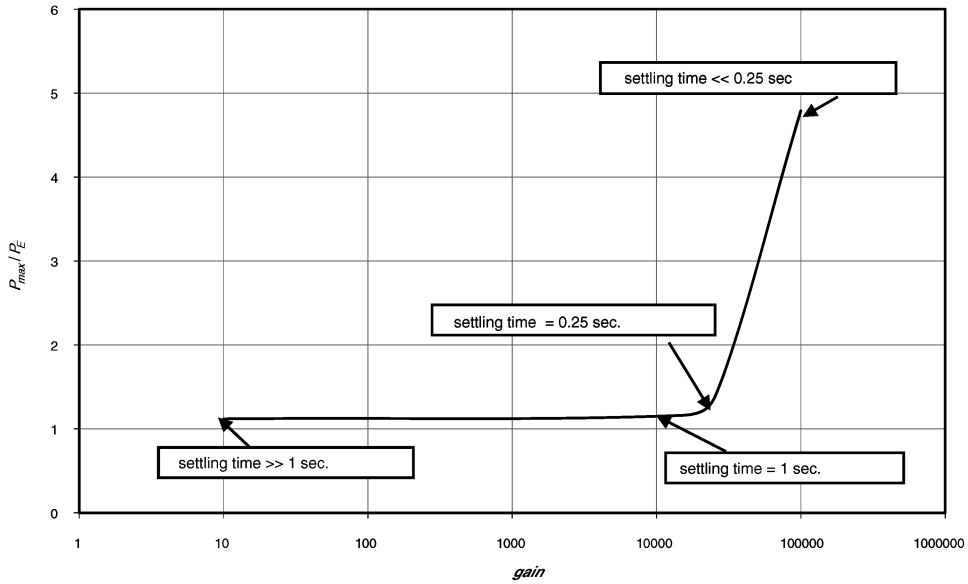

Fig. 4 Critical load enhancement with gain for a cantilevered column with $\beta_1 = 0$.

of the beam by a slight adjustment of its depth). This approach appears attractive, as it makes it possible to proceed with the analysis without a priori selection of the thickness. Once the analysis is complete, the designer will be able to select the thickness based on the feedback voltage considering alternative materials. In the final evaluation of the system performance the small additional mechanical contribution can be explicitly included as now the thickness is known.

F. Equations of Motion

Equating the internal virtual work to the external virtual work, we have

$$\int_{x=0}^{L} \{\bar{m}\,\ddot{v}\}\delta v\,\mathrm{d}x + EI\int_0^L \frac{\mathrm{d}^2 v}{\mathrm{d}x^2}\frac{\mathrm{d}^2(\delta v)}{\mathrm{d}x^2}\,\mathrm{d}x - P\int_0^L \frac{\mathrm{d}v}{\mathrm{d}x}\frac{\mathrm{d}(\delta v)}{\mathrm{d}x}\,\mathrm{d}x + \frac{EI}{L^2}\left\{\left[\beta_1\left(\frac{v}{L}\right) + \beta_3\left(\frac{v}{L}\right)^3\right](\delta v)\right\}_{x=L} + P\left\{\frac{\mathrm{d}v}{\mathrm{d}x}(\delta v)\right\}_{x=L} + 2E_P e_p \frac{h}{2} b_P \int_x V(x)\frac{\mathrm{d}^2(\delta v)}{\mathrm{d}x^2}\,\mathrm{d}x = \int_0^L q(x)\cdot\delta v\,\mathrm{d}x \qquad (17)$$

where

$$\beta_1 = K_1\frac{L^3}{EI}$$

and

$$\beta_3 = K_3\frac{L^5}{EI}$$

where β_1 and β_3 are dimensionless. Note that a dot denotes differentiation with respect to t, the time. A set of ordinary differential equations in time domain are derived from Eq. (17) by expressing v in terms of, say, N generalized coordinates v_i and associated shape functions ϕ_i satisfying the kinematic constraints of the cantilever at $x = 0$, that is,

$$v = \sum_{i=1}^{N} v_i\phi_i(x) \qquad (18)$$

The voltage distribution is taken in a similar form

$$V = \sum_{i=1}^{N} V_i\psi_i(x) \qquad (19)$$

Note the following:

1) Unlike in Eq. (18), x ranges over the length of the piezoelectric patch only in Eq. (19) and $V = 0$ outside this range.

2) Though the present treatment is based on an assumption of continuous piezoelectric patch and voltage as a continuous function of x, short discrete patches with small gaps between them need to be used in actual implementation to eliminate electric current flow in the longitudinal direction. The lateral load is considered to be uniformly distributed and equal to q_o per unit length.

Thus, the equations of motion take the form

$$M_{ij}\ddot{v}_j + \lfloor A_{ij} - PB_{ij} + PC_{ij}\rfloor v_j + A_{ijkl}v_j v_k v_l + E_{ij}V_j = q_i \qquad (20)$$

where

$$M_{ij} = \bar{m}\int_0^L \phi_i\phi_j\,\mathrm{d}x \qquad (21a)$$

Table 1 Maximum load and corresponding voltage for stable response (linear)

Gain	Maximum load attained $P_{\max}/P_E$	Maximum load attained $P_{\max}/P_{\mathrm{cr}}$	Maximum voltage recorded, V
		$\beta_1 = 0$	
0.0	2.04	1.0	0.0
10.0	1.12	0.5490	0.2
1.0E4	1.15	0.5637	99.3
2.5E4	1.36	0.6667	203.0
10.0E4	4.79	2.3480	392.9
		$\beta_1 = 30$	
0.0	3.63	1	0
10.0	3.46	0.9532	0.14
1.0E4	3.65	1.0055	78.33
2.5E4	3.87	1.0661	153.89
10.0E4	3.98	1.0964	483.4
		$\beta_1 = 36$	
0.0	3.93	1	0
10.0	3.1	0.788804	0.124
1.0E4	3.1	0.788804	79.18
2.5E4	3.1	0.788804	157.04
10.0E4	3.1	0.788804	504.68
		$\beta_1 = 120$	
0.0	2.23	1	0
10.0	2.23	1	0.067
1.0E4	2.23	1	19.98
2.5E4	2.23	1	48.5
10.0E4	2.23	1	170.9

$$A_{ij} = EI\int_0^L \phi_i''\phi_j''\,\mathrm{d}x + \frac{EI}{L^3}\beta_1(\phi_i\phi_j)_{x=L} \tag{21b}$$

$$B_{ij} = \int_0^L \phi_i'\phi_j'\,\mathrm{d}x \tag{21c}$$

$$C_{ij} = (\phi_i\phi_j')_{x=L} \tag{21d}$$

$$E_{ij} = 2E_P e_P \frac{h}{2} b_P \int_0^L \phi_i''\psi_j\,\mathrm{d}x \tag{21e}$$

$$q_i = q_o\int_0^L \phi_i\,\mathrm{d}x \tag{21f}$$

$$A_{ijkl} = \frac{EI}{L^5}\beta_3(\phi_i\phi_j\phi_k\phi_l)_{x=L} \qquad (i,j,k,l = 1,\ldots,N) \tag{21g}$$

Note that the matrix C_{ij} is asymmetric. The shape functions $\phi_i(x)$ are selected to be

$$\phi_i(x) = 1 - \cos\left(\frac{i\pi x}{L}\right) \qquad (i = 1,3,\ldots,N) \tag{22}$$

Thus, we have

$$\delta\varepsilon|_{z=\pm\frac{h}{2}} = \mp\frac{h}{2}\cdot\frac{\mathrm{d}^2(\delta v)}{\mathrm{d}x^2} = \mp\frac{h}{2}\cdot\delta v_i\phi_i'' = \mp\frac{h}{2}\sum_{i=1,3\ldots,}^{N}\left\{\left(\frac{i\pi}{2L}\right)^2\cdot\cos\left(\frac{i\pi x}{2L}\right)\right\}\cdot\delta v_i \tag{23}$$

G. Feedback Control

Letting the feedback voltage be proportional to the flexural strain rate, we have

$$V = G\frac{h}{2}\cdot\frac{\mathrm{d}^2\dot{v}}{\mathrm{d}x^2} = G\frac{h}{2}\sum_{i=1,3\ldots,}^{N}\dot{v}_i\left(\frac{i\pi}{2L}\right)^2\cdot\cos\left(\frac{i\pi x}{2L}\right) \tag{24}$$

where G is the gain. Thus,

$$V = \sum_{i=1,3\ldots,}^{N} V_i\cos\left(\frac{i\pi x}{2L}\right) \tag{25}$$

where

$$V_i = \frac{h}{2}G\left(\frac{i\pi}{2L}\right)^2\dot{v}_i \qquad \text{(no sum on } i\text{)} \tag{26}$$

Then the piezoelectric term $E_{ij}V_j$ on the left-hand side of Eq. (20) can be written (suspending the index notation) in the form

$$E_{ij}V_j = 2E_p e_p G b_p\left(\frac{h}{2}\right)^2\left(\frac{i\pi}{2L}\right)^2\sum_{j=1,3\ldots,}^{N}\left(\frac{j\pi}{2L}\right)^2\dot{v}_j\int_x\cos\left(\frac{i\pi x}{2L}\right)\cdot\cos\left(\frac{j\pi x}{2L}\right)\mathrm{d}x \tag{27}$$

The integration is over the length of the patch. This expression may be abbreviated as $D_{ij}\dot{v}_j$. Note if the patches run from end to end, the D matrix is diagonal. Importantly, the piezoelectric term [Eq. (27)] in the governing equations [Eq. (20)] may be viewed as controlled by a single system parameter $E_p e_p G$ (i.e., the system response to given external loading is unaffected as long this is kept constant). Voltages [vide Eq. (24)], of course, will be proportional to G.

The final equations take the form

$$M_{ij}\ddot{v}_j + D_{ij}\dot{v}_j + \lfloor A_{ij} - PB_{ij} + PC_{ij}\rfloor v_j + A_{ijkl}v_j v_k v_l = q_i \tag{28}$$

III. Results and Discussion

The following aspects of stability and control of the cantilevered column are studied in this paper: 1) relationship between the control

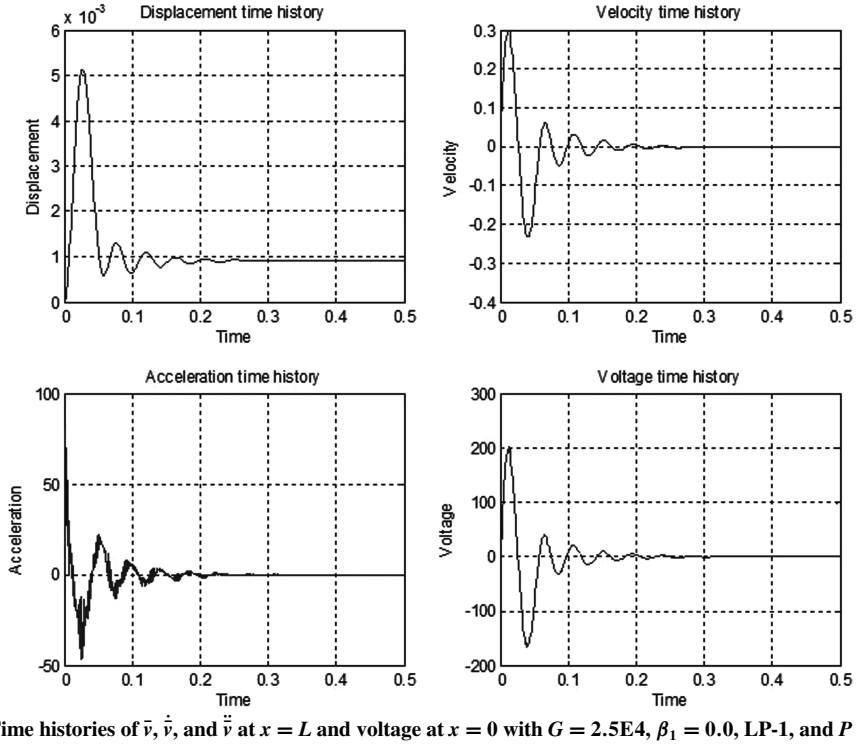

Fig. 5 Time histories of $\bar{v}$, $\dot{\bar{v}}$, and $\ddot{\bar{v}}$ at $x = L$ and voltage at $x = 0$ with $G = 2.5\text{E}4$, $\beta_1 = 0.0$, LP-1, and $P = 2P_{cr}/3$.

gain and the maximum load attainable over the entire range of spring stiffness, 2) effect of loading sequence, 3) influence of spring nonlinearity, and 4) relative merits of partial over full-patch control.

A. Linear Behavior of Uncontrolled Column

First consider the instability problem given by the linear homogeneous equation by setting D_{ij}, A_{ijkl} and q_i to zero in Eq. (28). The critical values of the axial load can be obtained incrementing P in small steps and solving the linear eigenvalue problem obtained by taking $v_i = A_i e^{\lambda t}$. The lowest critical values of P obtained thereby may correspond to flutter (a root for λ has a positive real part and a nonzero imaginary part) or divergence (a root is real and positive). These results are plotted in Fig. 2 in terms of the nondimensional load parameter $p = P_{\max}/P_E$ (where $P_E = \pi^2 EI/L^2$) and the nondimensional linear spring stiffness β_1. The latter varies from 0 to 140 as shown in, Fig. 2. These results are in very close agreement with those obtained by Wang and Quek [1]. There are three ranges of spring stiffness, each of which correspond to a characteristic mode of column response [viz., flutter range ($0 < \beta_1 < 36$), transition range ($36 < \beta_1 < 40$), and divergence (buckling) range ($\beta_1 > 40$)]. The remarkable features of the p versus β_1 relationship (Fig. 2) are the abruptness of the transition and the drop in the critical load with increasing spring stiffness.

B. Numerical Study of Controlled Column Response

The eigenvalue analysis is continued to be employed in further work to compute maximum loads attainable for a prescribed gain by including $D_{ij}\dot{v}_j$ in Eq. (28). However, such analysis does not give us any hint of the actual performance of the column and the control system as the critical load is approached in the presence of disturbances. In particular, it does not give the voltages that must develop across the piezopatches for a given program of loading. To illustrate the effectiveness of piezoelectric control and the voltages developed in the context of a given disturbance, we consider a column having specific geometric and material properties.

1. Geometry of the Host Beam

$L = 1000$ mm; cross section: width, $b = 50$ mm, depth, $h=$ 20 mm; mass per unit length $= 2700\ \mathrm{kg\,m^{-3}}$; host beam $E=$ 63 GPa.

Selection of Piezoelectric Material

New piezoelectric materials with ever-increasing values of e_P (d_{31}) are being currently introduced (e.g., 180×10^{-12} $\mathrm{mV^{-1}}$ for PZT5A to 370 $\mathrm{mV^{-1}} \times 10^{-12}$ for PZT5) [16]. The value of E_p may be taken as 63 GPa for this family of materials. The product $E_p e_p$ (with units of $\mathrm{NV^{-1}mm^{-1}}$) takes on values of 0.0113 and 0.0233, respectively. In the present study, we select a benchmark value $E_p e_p$ as 0.0283 to be in line with earlier work [2]. Apparently this value is on the higher end of the spectrum. If the actual value of $E_p e_p$ is smaller, say, one-half of this value (0.01415), the results quoted here will still be applicable provided the gain G and the corresponding voltages are doubled. This would, in some cases, call for a higher thickness of the piezoelectric patch as there is a limit to the field strength the material can withstand.

Perturbation to Trigger Dynamics

Consider a perturbation in the form of uniformly distributed force q_o per unit length. (The manner of application is discussed later.) The magnitude of q_o is taken as proportional to the critical load of the uncontrolled column (which is function of β_1) in the form $q_o = kP_{\mathrm{cr}}/L$. k is selected such that the column with no axial load and no spring ($p = \beta_1 = 0$) has a maximum dynamic deflection of 1% of its length (10 mm) and is found to be 2.055×10^{-3}.

Solution Procedure

The set of Eq. (28) is solved using Newmark–β method in conjunction with Newton–Raphson iterative procedure when nonlinearity is present [2]. Accuracy of the solution is checked varying the value of N and the time step; it was found that sufficiently accurate results could be obtained taking $N = 9$. Time step needs to be a small fraction of the smallest of the time periods of modes of vibration involved. The accuracy of the numerical results was also checked by comparing the results of $P_{\max}$ for vanishingly small disturbances with those of the eigenvalue analysis.

C. Behavior and Control of Column with Linear Spring

The linear problem is considered first setting $\beta_3 = 0$. As before, β_1 varies from 0 to 140. The column is actuated by a double piezoelectric patch covering the entire span. Three values of gain G (with $E_p e_p = 0.0283$) are selected for investigation: case 1, $G = 0$

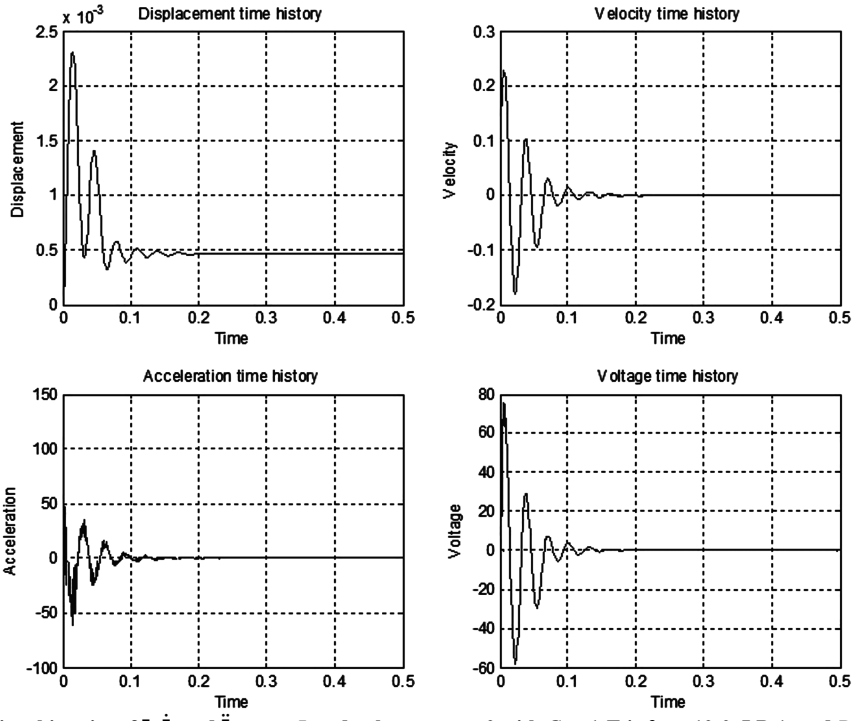

Fig. 6 Time histories of $\bar{v}$, $\dot{\bar{v}}$, and $\ddot{\bar{v}}$ at $x = L$ and voltage at $x = 0$ with $G = 1.E4$, $\beta_1 = 10.0$, LP-1, and $P = 2P_{\mathrm{cr}}/3$.

[i.e., uncontrolled (undamped) column]; case 2, $G = 10$, a very small gain; and case 3, $G = 2.5 \times 10^4$, representative of values likely to be used in practical applications.

1. Small Damping Effect

First we consider the column propped by a linear spring ($\beta_1 \geq 0$, $\beta_3 = 0$, and $q = 0$) with a feedback control given by $G = 10$ (case 2). This is a case of small gain, as it will be shown that with this gain the control voltages across the patches turn out to be very small in comparison to case 3, under the selected disturbance. The corresponding linear eigenvalue problem is solved repeatedly with the follower force P incremented in small steps, until the threshold instability is reached as shown in Fig. 3. This load is designated as $P_{\max}$ to distinguish it from the maximum load $P_{\rm cr}$ for the case $G = 0$.

It is important to note that in this case, the maximum load in fact decreases significantly from that corresponding to case 1 in the flutter range. This is consistent with the well-known effect of small viscous

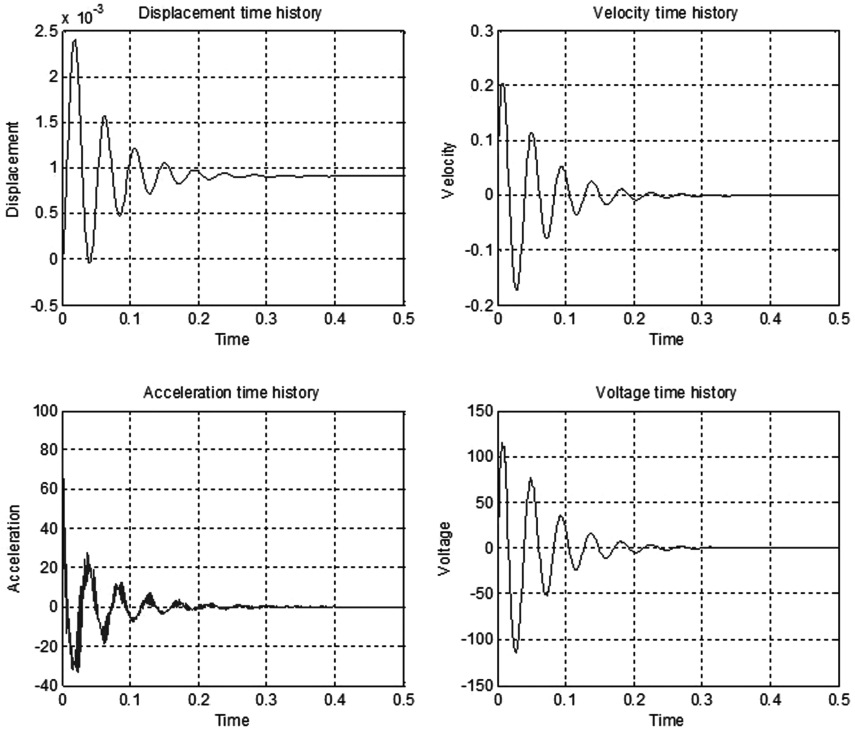

Fig. 7 Time histories of $\bar{v}$, $\dot{\bar{v}}$, and $\ddot{\bar{v}}$ at $x = L$ and voltage at $x = 0$ with $G = 1.E4$, $\beta_1 = 10.0$, LP-2, and $P = 2P_{\rm cr}/3$.

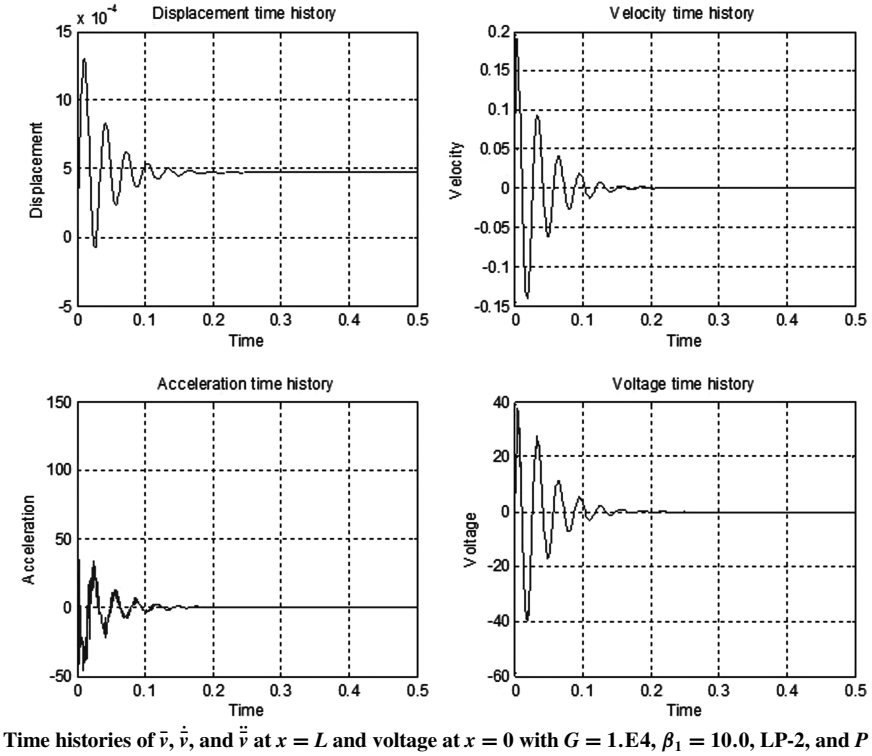

Fig. 8 Time histories of $\bar{v}$, $\dot{\bar{v}}$, and $\ddot{\bar{v}}$ at $x = L$ and voltage at $x = 0$ with $G = 1.E4$, $\beta_1 = 10.0$, LP-2, and $P = 2P_{\rm cr}/3$.

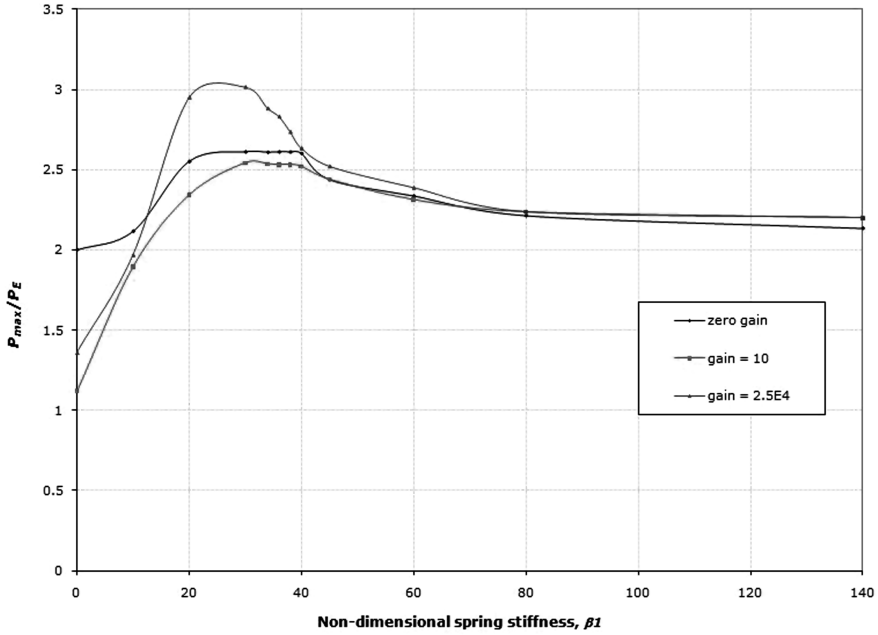

Fig. 9 Effect of nonlinearity and gain on the load-carrying capacity.

damping in linear circulatory systems [17,18]. Such systems must always be analyzed with some damping taken into account to avoid nonconservative results. Thus, the results for the case of gain $G = 10$ should be taken as truly representative of the uncontrolled column.

The case with $\beta_1 = 0$ is particularly interesting. The drop in the critical load from that for the case 1 is significant (42%). Significant drops in the critical loads are seen in the flutter range up to $\beta_1 \approx 10$. This effect becomes less significant as the spring stiffness increases and vanishes as the buckling range is approached.

2. *Critical Load Enhancement*

Figure 3 also plots the critical load attainable when the gain, G is increased to 2.5×10^4. Significant enhancements (of about 50% in some cases) in the critical loads are seen throughout the flutter range, but this would come at the expense of significant increases in the voltages across the patches in the context of a specified disturbance: a point that is discussed in the sequel. Figure 4 plots the critical load attainable for various values of gain for the case with $\beta_1 = 0$. As the gain is increased from 10^4 to 10^5, the load-carrying capacity increases abruptly.

However, in the transitional range (Fig. 3) and beyond ($\beta_1 > 30$), the velocity dependent feedback control (considered in the present study) cannot and does not enhance the critical load [5]. With $G = 2.5 \times 10^4$, the maximum critical load over the entire range of β_1 occurs at a value of $\beta_1 = 20$ and this corresponds to an enhancement of the critical load by about 35% from case 1 and 43% from case 2.

3. *System Performance*

The following loading sequences are considered:

1) In loading program LP-1, the follower force and lateral loading are ramped up simultaneously in duration of 0.07 s to reach their respective chosen values (viz., P and q) and remain unchanged thereafter.

2) In loading program LP-2, the follower force is preset at the specified value of P and the lateral force q is then suddenly applied: a Heaviside step function of time.

LP-1 is the preferred loading program in the present study as it will be seen to more adverse: a point discussed in the sequel. The dynamic performance is studied by systematically increasing P till a preset value is attained. The analysis is repeated till the onset of dynamic instability. The maximum voltages (recorded at the clamped end) just within dynamic instability are given in the Table 1 for values of β_1 (viz,. 0, 30, 36, and 120, respectively). The cases with $\beta_1 = 0$ and 30 are of particular interest in that the voltage increases are accompanied by significant increases in the follower force that can be carried. For other cases, such enhancement of the critical load is either marginal or nonexistent. The maximum voltages recorded across the piezoelectric patches for all the cases increase rapidly with the gains selected. Note that the case 2 with $G = 10$ is associated with very small voltages, whereas significant reductions occur in the load-carrying capacity.

From the point of view of limiting the thickness of piezoelectric patches, it is desirable to keep the maximum voltages as small as possible while at the same time enhancing the load-carrying capacity. Because these voltages are attained as soon as the disturbance is felt by the column, it is possible to minimize these by choosing a smaller gain in the first few milliseconds and ramping up the gains rapidly beyond that. However, this was not tried in the present study. Below the critical load the column is completely controllable and this is illustrated in several cases (Figs. 5–8) for cases with $\beta_1 = 0$ and 10 and under LP-1 and LP-2.

Table 2 Maximum load and corresponding voltage for stable response (nonlinear)

Gain	Maximum load attained		Maximum voltage recorded, V
	$P_{\max}/P_E$	$P_{\max}/P_{\text{cr}}$	
		$\beta_1 = 30$	
0.0	3.63	1	0
10.0	2.7225	0.75	0.212
1.0E4	2.9766	0.82	89.724
2.5E4	3.0129	0.83	181.09
10.0E4	3.4122	0.94	529.54
		$\beta_1 = 36$	
0.0	3.93	1	0
10.0	2.6724	0.68	0.21
1.0E4	2.751	0.7	91.61
2.5E4	2.8296	0.72	180.73
10.0E4	2.8296	0.72	552.87
		$\beta_1 = 120$	
0.0	2.23	1	0
10.0	2.0962	0.94	0.126
1.0E4	2.1408	0.96	31.18
2.5E4	2.1408	0.96	62.08
10.0E4	2.1408	0.96	187.58

4. Significant Role of the Spring

The addition of a relatively light spring significantly enhances the load-carrying capacity of the column and this enhancement increases with the gain, G, selected. Considering the case of $G = 10$, the addition of a relatively light spring ($\beta_1 = 10$) enhances the load-carrying capacity significantly: a 90% increase occurs (Fig. 3). Also, for the standard perturbing force selected, the column with $\beta_1 = 10$ requires a smaller gain and a drastically reduced voltage demand for a given settling time. This is illustrated in Figs. 5 and 6, where the time history responses, respectively, of a cantilever without the spring and those with a spring with $\beta_1 = 10$ under LP-1 are shown. Note that here and in subsequent figures, the plots are for $\bar{v}$, $\dot{\bar{v}}$, and $\ddot{\bar{v}}$, which are dimensionless quantities defined by

$$\{\bar{v}, \dot{\bar{v}}, \ddot{\bar{v}}\} = \left\{\frac{v}{L}, \frac{\dot{v}}{L}, \frac{\ddot{v}}{L}\right\}_{x=L} \tag{29}$$

A value of P equal to $2P_{cr}/3$ (P_{cr} is the critical value of P for the uncontrolled, undamped column) is selected in each case to represent a working condition with 50% margin of safety. However, it turns out that for the case with $\beta_1 = 0$, this exceeds the maximum load unless a gain of 2.5E4 is selected. For this gain, control is found to be effective with a settling time of 0.2 s. Now compare this with the column having $\beta_1 = 10$. For a settling time less than 0.2 s, the gain required (1.0E4 versus 2.5E4) and the voltage demand are both 40% of those required for $\beta_1 = 0$.

5. Effect of Loading Sequence

The maximum values of the displacements, velocities, and voltages developed depend upon the sequence of application of the follower force, P and lateral load, q. The time histories for columns with $\beta_1 = 0$ and $\beta_1 = 10$ subjected to LP-2 are presented in Figs. 7 and 8, respectively. These are compared with, respectively, with Figs. 5 and 6, which plot time histories for LP-1. It is seen that under LP-2, the maximum displacements as well as the maximum voltages developed are significantly smaller than in LP-1. The reason for this is not far to seek. The follower force has a transverse component, which tends to reduce the column displacements. This effect is available in full at the instant the column is disturbed for LP-2 and hence the aforementioned reductions. Thus, LP-1 is seen to be more adverse and is used in the present study in order to be conservative.

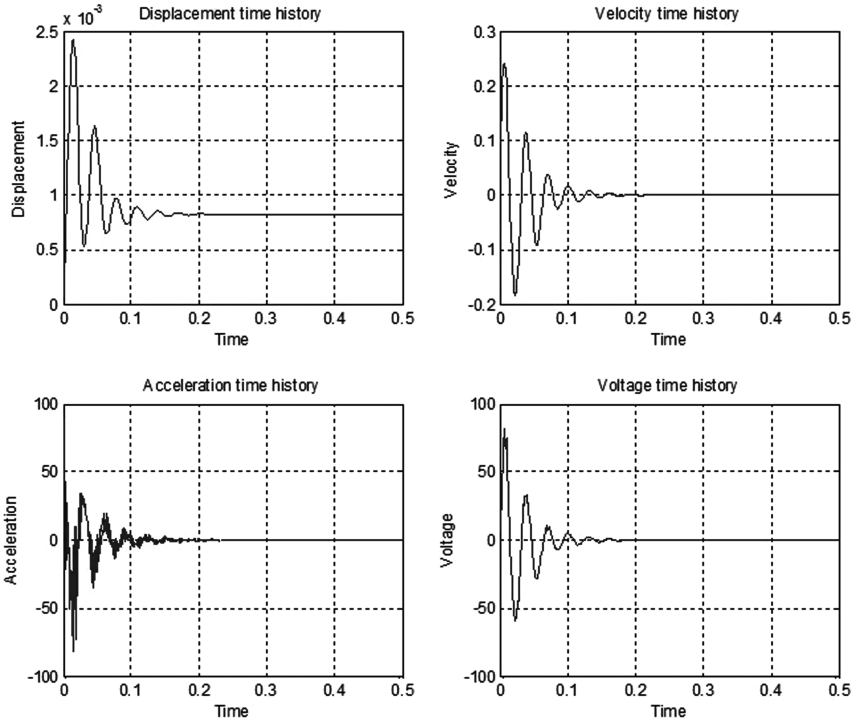

Fig. 10 Time histories of $\bar{v}$, $\dot{\bar{v}}$, and $\ddot{\bar{v}}$ at $x = L$ and voltage at $x = 0$ with $G = 1.E4$, $\beta_1 = 10.0$, $\beta_3 = -2000$, LP-1, and $P = 2P_{cr}/3$.

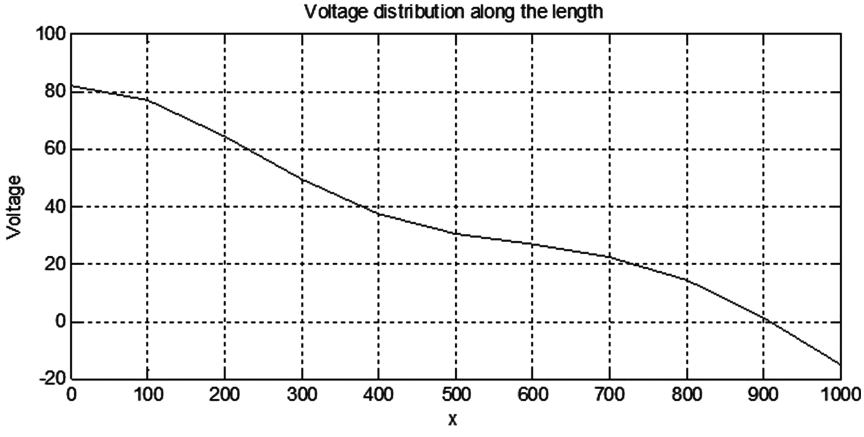

Fig. 11 Voltage distribution along the length (at $t = 0.011$ s).

6. Nonlinear Case

Next consider the problem where the spring has a softening nonlinearity given by $\beta_3 = -2000$. The spring nonlinearity is such as to cause a reduction of the force carried by 20% from that sustained by a linear spring when the spring undergoes a deflection of 10 mm ($\delta = L/100$). The effect of nonlinearity on the load-carrying capacity is illustrated in Fig. 9, which shows a relationship between the maximum follower force P that can be carried by the column and the spring stiffness β_1 for three differing values of gain under LP-1.

The relationship for the nonlinear spring differs significantly from that of the linear spring (Fig. 3) in one significant respect. The steep increase of $P_{\max}/P_E$ with β_1 in the flutter range and its subsequent steep drop in the transition range is replaced by a more rounded characteristic with the critical loads attained significantly reduced from those of the linear case. As spring stiffness increases beyond this range, the nonlinearity has a minimal effect as the deflections suffered by the spring become smaller and smaller. Table 2 lists the maximum loads that can be attained with these gains and the maximum voltages that develop for three values of β_1 (viz., 30, 36, and 120). Piezoelectric actuation with the higher gain ($G = 2.5\text{E}4$) once again is seen to enhance the critical loads from the values corresponding to small gain case (with $G = 10$). However, significant increases are seen only in the flutter and transitional range and the percentage enhancements are similar to that seen in the linear case. The optimal spring stiffness is still about 20, though the corresponding maximum load that can be attained with control suffers a reduction because of nonlinearity and the voltages required for control are higher. Thus, whereas the addition of the spring does improve the system performance, it is important to consider carefully the nonlinearity, if any that may exist.

Figure 10 gives time histories of a column with $\beta_1 = 10$, $\beta_3 = -2000$, $P = 2P_{\text{cr}}/3$, and $G = 1.\text{E}4$ under LP-1. A comparison with Fig. 6, which plots the same for the case with $\beta_3 = 0$ (linear case), brings out the influence of nonlinearity. It is seen that the maximum displacement and velocity at the propped end as well as the maximum voltage at the fixed end are significantly higher.

7. Partial Patch Control

Figure 11 illustrates the variation of voltage along the column length ($\beta_1 = 0$) with $P = 2P_{\text{cr}}/3$ (gain = 1.E4) subjected to LP-1 at the instant when the maximum voltage is recorded at the fixed end. It is clear that the voltage distribution is nonuniform; the highest intensity of voltages occur in the portion of the column given by $0 < x < L/2$ [i.e., from the fixed end to midspan ($x = L/2$)] and tends to taper off in the right half of the column. Such variation of

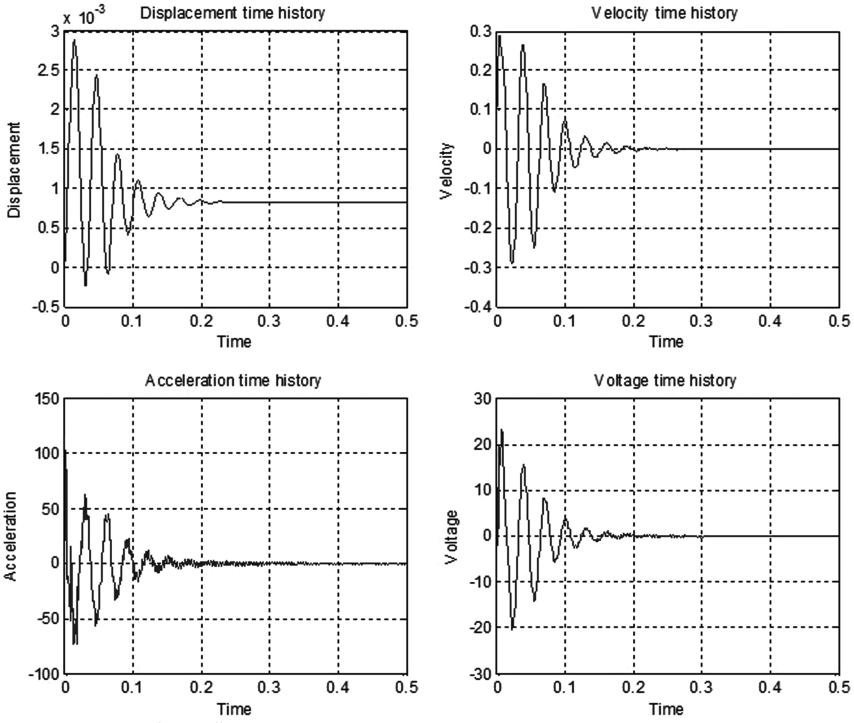

Fig. 12 Time histories of $\bar{v}$, $\dot{\bar{v}}$, and $\ddot{\bar{v}}$ at $x = L/2$ and voltage at $x = 0$ with $G = 1.\text{E}3$, $\beta_1 = 10.0$, LP-1, and $P = 2P_{\text{cr}}/3$.

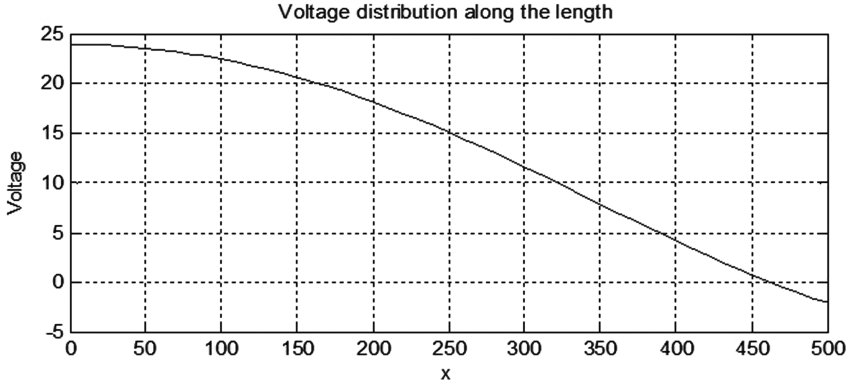

Fig. 13 Voltage distribution along the length of the piezopatch at 0.08 s (half-piezopatch with $G = 1.\text{E}3$, $\beta_1 = 10.0$, and $P = 2P_{\text{cr}}/3$).

voltage is typical for columns with relatively light springs with β_1 falling within the flutter range. Given this voltage distribution it appears that the column can be controlled by a double piezopatch covering a fraction of the column length from the fixed end. In the present study, the column is sought to be controlled with such piezopatches spanning one-half, one-third, and one-quarter of the length of the column.

8. *Half-Piezopatch*

Consider the column with $\beta_1 = 10$ carrying a follower force of $2P_{\text{cr}}/3$ subjected to LP-1. It can be seen from Fig. 3 that to attain this load, a gain of 1×10^4 was required (also refer to Fig. 7 for the time histories). Figure 12 plots the time histories for the same column but with half-piezopatch. With half-patch, a smaller gain of 1000 is found to be adequate. The maximum voltage attained is much smaller (23.5 V vs 75 V of the full-patch case) and the settling time is smaller as well (0.18 s vs 0.2 s). Voltage distribution at an instant when the highest value is attained is shown in Fig. 13. Once again, the voltage is concentrated in the region close to clamped end.

With a view to probe further into the relative efficacy of half-patch control over the full-patch control, the critical load capacities were obtained for the entire range of β_1 values with two representative values of gain (viz., 10 and 1000). The results are shown in Fig. 14 along with those for zero gain. Comparing these results with those in Fig. 3, the critical limits are higher with half-patch $\beta_1 < 25$,

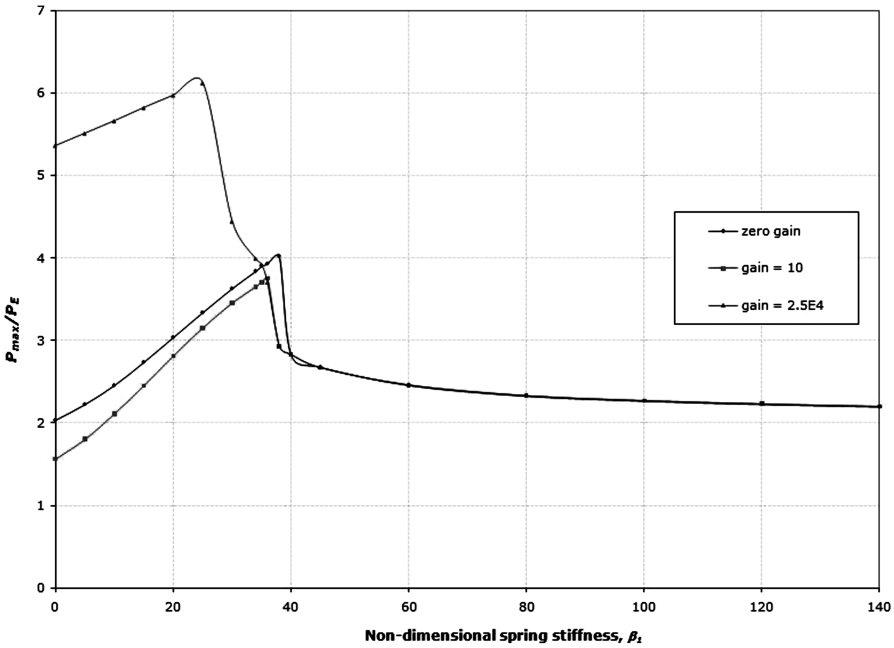

Fig. 14 Critical limit using half-patch (0 to $L/2$).

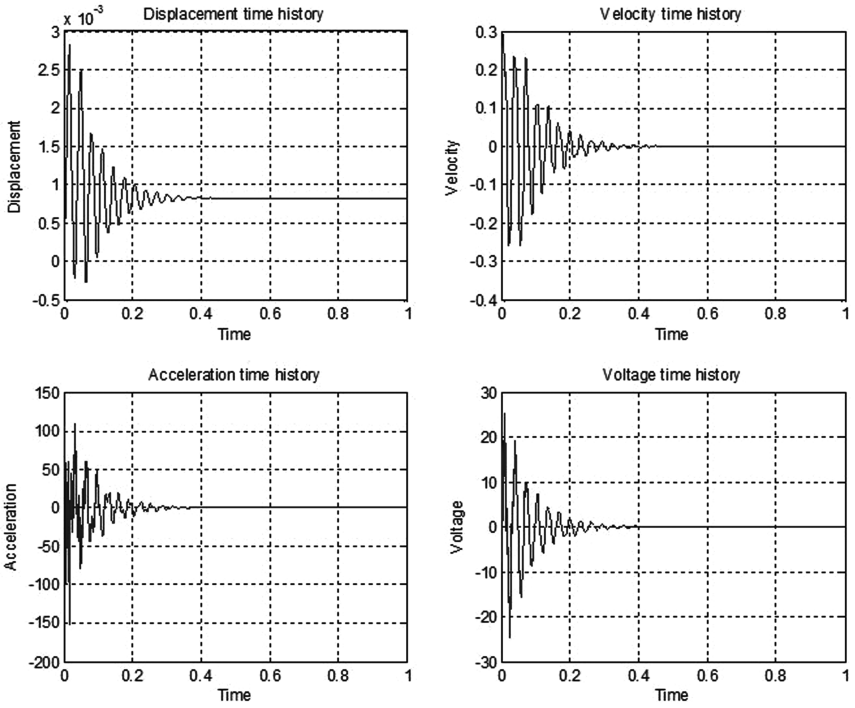

Fig. 15 One-third piezopatch: time histories of $\bar{v}$, $\dot{\bar{v}}$, and $\ddot{\bar{v}}$ at $x = L/3$ and voltage at $x = 0$ with $G = 2.\text{E}3$, $\beta_1 = 10.0$, LP-1, and $P = 2P_{\text{cr}}/3$.

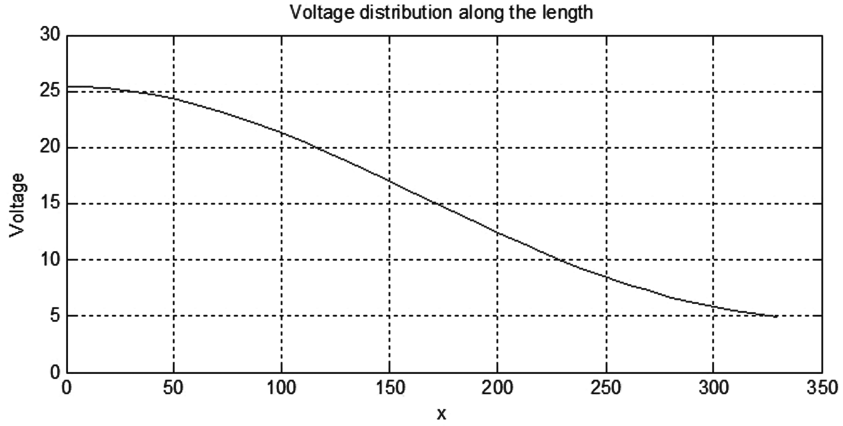

Fig. 16 Voltage distribution along the length of one-third patch at 0.09 s.

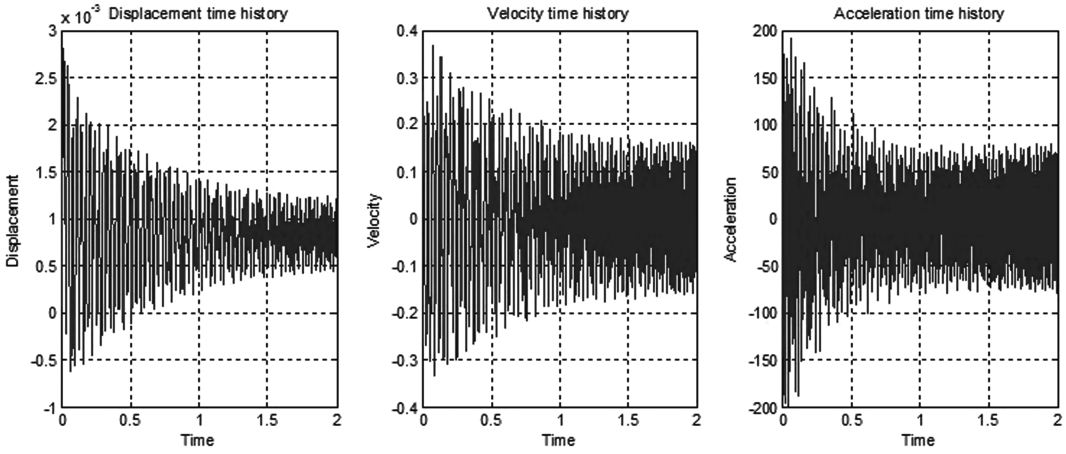

Fig. 17 Case 1: time histories of $\bar{v}$, $\dot{\bar{v}}$, and $\ddot{\bar{v}}$ at $x = L$ with $G = 2.5.E4$, $\beta_1 = 10.0$, LP-1, and $P = 2P_{cr}/3$.

indicating that the half-patch control is more effective in the flutter range. Neither the full-patch nor the half-patch control are effective in enhancing the critical load in the buckling range for the negative velocity-based feedback control employed in the present study.

9. *Patches of Smaller Length*

The same example illustrated in Fig. 12 ($\beta_1 = 10$, $G = 1.E3$, $P = 2P_{cr}/3$, and LP-1) is studied with a piezopatch applied from the fixed end to one-third of its length. The results are shown in Fig. 15. The maximum voltage required is 25.3 V, which is slightly higher than the half-patch case. The settling time for this case is about 0.5 s. This is better than the full-patch case where no control is possible for $G = 2.E3$, but certainly is less efficient than the half-patch control. Voltage distribution when the peak value is attained is shown in Fig. 16. When the patch length is reduced to $L/4$, no control is possible for the parameters chosen.

10. *Three Piezopatches*

To gain further insight into the most advantageous distribution of patches, the column was sought to be controlled with three patches. The following cases were studied:

In case 1, three equal-sized patches are tried with the following parameters: patch width 200 mm ($L/5$), $G = 2.5E4$, $\beta_1 = 10$, and LP-1. Table 3 gives the width and the location of patches.

The time histories of v, $\dot{v}$, and $\ddot{v}$ at $x = L$ are shown in Fig. 17 and the histories of voltage at the center of patches are shown in Fig. 18. The oscillations become steady with no hint of getting damped as do the patch voltages at the end of 2 s. It is clear that the strategy has failed.

In case 2, the next attempt involved varying the widths of the patches and locating the higher-width patches closer to the clamped end. [The other parameters were kept unchanged (i.e., $G = 2.5E4$, $\beta_1 = 10$, and LP-1).] The patch widths and the corresponding distances from the clamped end (x coordinates of the center of patch) are given in Table 3.

The time histories corresponding to $x = L$ are shown in Fig. 19. Though there is a gradual reduction of the displacements, velocities, and accelerations, these take an inordinately long time to get damped out. Also, the controlling maximum voltages in patches are high (Fig. 20) relative to half-patch case. All the three patches record roughly the same maximum voltage of 253 V.

11. *Two Piezopatches*

To examine the role of the third patch away from the clamped end, case 2 is studied with the third patch removed. The time histories of

Table 3 Location of piezopatches

Patch number	Patch width, mm	X coordinate of the center of patch, mm
	Case 1	
1	200	100
2	200	500
3	200	900
	Case 2	
1	300	150
2	200	500
3	100	950

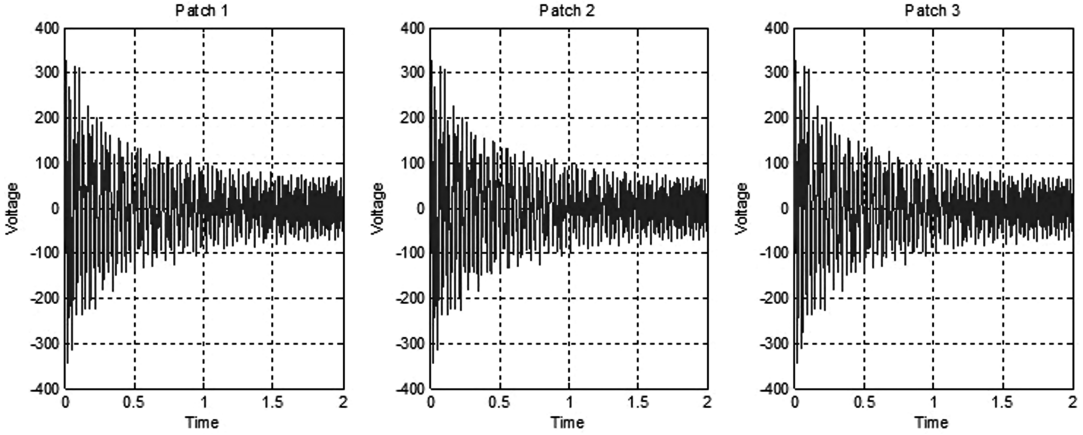

Fig. 18 Case 1: voltage time histories of each patch (voltages correspond to middle of each patch).

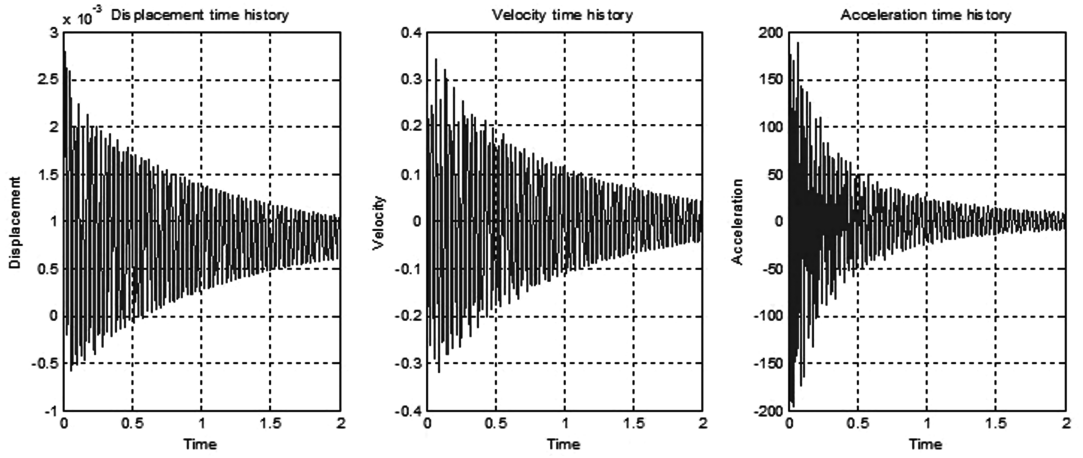

Fig. 19 Case 2: time histories of $\bar{v}$, $\dot{\bar{v}}$, and $\ddot{\bar{v}}$ at $x = L$ with $G = 2.5\text{E}4$, $\beta_1 = 10.0$, LP-1, and $P = 2P_{\text{cr}}/3$.

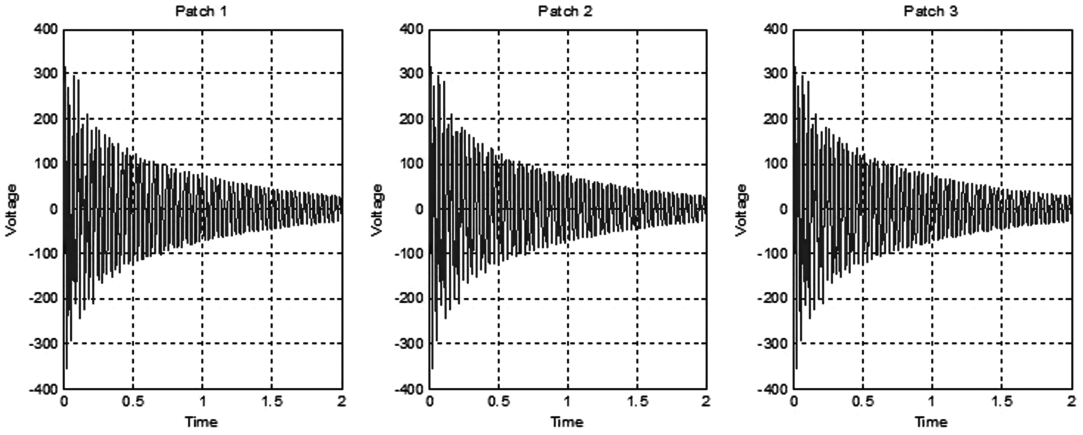

Fig. 20 Voltage time histories of each patch for case 2 (voltages correspond to middle of each patch).

displacement, velocity, and accelerations are identical to the three patch case as shown in Fig. 19. Even the voltage time histories for patches 1 and 2 are same as those in Fig. 20. Thus, it is seen that the third patch near the propped end does not appear to perform any useful role.

IV. Conclusions

1) The critical loads of a column carrying a follower force can be enhanced significantly by piezoelectric control with feedback voltages proportional to the bending strain rates. The feasibility of employing such control is demonstrated by computing the voltages that must develop across the piezopatches when the column is subjected to a typical disturbance. Whereas selecting a high gain can ensure a desired enhancement in the critical load, the voltages developed across the piezopatches may turn out to be unacceptably high.

2) The critical loads obtained with zero gain (with no piezoelectric control and no viscous damping) have limited practical significance in the flutter range. A small (but finite) value of gain must be incorporated in numerical analyses to obtain realistic estimates of critical load.

3) Provision of an elastic support (spring) at the free end of a clamped column can dramatically enhance the performance of both

the structure and the control system. There is an optimal spring stiffness that results in the highest critical load for a given gain and this stiffness lies in the range where flutter rather than divergence (buckling) is the mode of instability.

The stiffening of the column by the provision of a spring or some supporting structural element must be considered as part of the design concept, not something that can be introduced a posteriori. On the other hand, the active control technique may be employed to upgrade the capability of the structural element and may be appropriately designed to come into action just under overloads of relatively smaller frequency.

4) Careful consideration must be given to the sequence of loading of the follower force and lateral loading as this can affect the maximum displacements and voltages developed across the patches.

5) A moderate amount of softening nonlinearity has the effect of drastically rounding off the abrupt transition in the relationship between P_{cr} and β_1 (the linear spring stiffness) with or without control.

6) Control using a double piezopatch spanning only one-half of the column from the clamped end proved much more effective in terms of the higher critical loads that can be attained and the reduction in the voltages across the patches in comparison to control using piezopatches running from end to end. There is a limit to how short the patches can be for control to be effective or even possible.

7) Control schemes with patches distributed over the entire column were found to be not efficient in controlling flutter. Patches located away from the clamped end are completely ineffective in flutter control.

References

[1] Wang, Q., and Quek, S. T., "Enhancing Flutter and Buckling Capacity of Column by Piezoelectric Layers," *International Journal of Solids and Structures*, Vol. 39, No. 16, 2002, pp. 4167–4180. doi:10.1016/S0020-7683(02)00334-7

[2] Sridharan, S., and Kim, S., "Piezoelectric Control of Columns Prone to Instabilities and Nonlinear Modal Interaction," *Smart Materials and Structures*, Vol. 17, No. 3, 2008.

[3] Mukherjee, A., and Chaudhuri, A. S., "Active Control of Piezolaminated Columns—Exact Solutions and Experimental Validation," *Smart Materials and Structures*, Vol. 14, No. 4, 2005, pp. 475–482. doi:10.1088/0964-1726/14/4/003

[4] Gu, H., and Song, G., "Active Vibration Suppression of a Flexible Beam with Piezoceramic Patches Using Robust Model Reference Control," *Smart Materials and Structures*, Vol. 16, No. 4, 2007, pp. 1453–1459. doi:10.1088/0964-1726/16/4/060

[5] Wang, Q., and Varadan, V. K., "Transition of the Buckling Load of Beams by the Use of Piezoelectric Layers," *Smart Materials and Structures*, Vol. 12, No. 5, 2003, pp. 696–702. doi:10.1088/0964-1726/12/5/305

[6] Wang, Q., "On Buckling of Column Structures with a Pair of Piezoelectric Layers," *Engineering Structures*, Vol. 24, No. 2, 2002, pp. 199–205. doi:10.1016/S0141-0296(01)00088-8

[7] Kumar, D. Nagendra, Raja, S., and Ikeda, T., "Active Vibration Control of Smart Plates With Partially Debonded Multilayered PZT Actuators," *Smart Materials and Structures*, Vol. 16, No. 5, 2007, pp. 1584–1594. doi:10.1088/0964-1726/16/5/012

[8] Bent, A. A., Hagwood, N. W., and Rodgers, J. P., "Anisotropic Actuation with Piezoelectric Fiber Composites," *Journal of Intelligent Material Systems and Structures*, Vol. 6, No. 3, 1995, pp. 338–349. doi:10.1177/1045389X9500600305

[9] Oh, Il-Kwon, "Thermopiezoelectric Nonlinear Dynamics of Active Piezolaminated Plates," *Smart Materials and Structures*, Vol. 14, No. 4, 2005, pp. 823–834. doi:10.1088/0964-1726/14/4/042

[10] Zhou, R. C., Mei, Chuh, and Hwang, Jen-Kuang, "Suppression of Nonlinear Panel Flutter at Supersonic Speeds and Elevated Temperatures," *AIAA Journal*, Vol. 34, No. 2, 1996, pp. 347–354. doi:10.2514/3.13070

[11] Abdel-Motagaly, K., Guo, X., Duan, B., and Mei, C., "Active Control of Nonlinear Panel Flutter Under Yawed Supersonic Flow," *AIAA Journal*, Vol. 43, No. 3, 2005, pp. 671–680. doi:10.2514/1.13840

[12] Peters, D. A., and Wu, J. J., "Asymptotic Solutions to a Stability Problem," *Journal of Sound and Vibration*, Vol. 59, No. 4, 1978, pp. 591–610. doi:10.1016/S0022-460X(78)80137-0

[13] Tiersten, H. F., *Linear Piezoelectric Plate Vibrations*, Plenum, New York, 1969.

[14] "IEEE Standard on Piezoelectricity," Inst. of Electrical and Electronics Engineers, ANSI/IEEE Std. 176-1987, Piscataway, NJ, Jan. 1988.

[15] Lam, K. Y., Peng, X. Q., and Reddy, J. N., "A Finite-Element Model for Piezoelectric Composite Laminates," *Smart Materials and Structures*, Vol. 6, No. 5, 1997, pp. 583–591. doi:10.1088/0964-1726/6/5/009

[16] Li, Q., Mei, C., and Huang, J. K., "Suppression of Thermal Postbuckling and Panel Flutter Motions Using Piezoelectric Actuators," *AIAA Journal*, Vol. 45, No. 8, 2007, pp. 1861–1873. doi:10.2514/1.28280

[17] Bolotin, V. V., *Nonconservative Problems of the Theory of Elastic Stability*, Macmillan, New York, 1963.

[18] Huseyin, K., *Vibrations and Stability of Multiple Parameter Systems*, Sijthoff & Noordhoff, Alphen aan den Rijn, The Netherlands, 1978.

J. Cooper
Associate Editor